

2. EXPLANATORY NOTES¹

Shipboard Scientific Party²

LOGGING WHILE DRILLING

Downhole logs measure the physical and chemical properties of formations adjacent to the borehole. Interpretation of these continuous, in situ measurements yields a mineralogic, lithologic, stratigraphic, and geophysical characterization of the site. Where downhole core recovery is incomplete, log data may serve as a proxy for physical properties and sedimentologic data. They also complement the discrete measurements obtained from cores and offer several advantages over core-based analyses in that logs are rapidly collected and represent continuous, in situ measurements of the formation.

Logging-while-drilling (LWD) operations were conducted successfully twice previously from the *JOIDES Resolution* (Shipley, Ogawa, Blum, et al., 1995; Silver, Kimura, Blum, et al., 1997). LWD services were provided by Schlumberger Anadrill Drilling Services through a contract with the Lamont-Doherty Earth Observatory Borehole Research Group (LDEO-BRG).

LWD measures in situ formation properties shortly after the drill bit penetrates a formation, with instruments that are located in the drill collars immediately above the drill bit. These measurements are made before the borehole is adversely affected by continued drilling or coring operations. In addition, LWD measurements are made while the drill string is moving, which reduces the chances of the bottom-hole assembly (BHA) becoming stuck in the hole.

The LWD System

The drill string was configured with the LWD tools located directly above the drill bit (Fig. 1). The Anadrill LWD tools used on Leg 171A (see Table 1 for terminology) consisted of a compensated dual resistivity (CDR) tool, including a spectral gamma-ray tool, and a compensated density neutron (CDN) tool (Wraight et al., 1989; Anadrill-Schlumberger, 1993; Desbrandes, 1994). The LWD equipment is battery powered and uses erasable/programmable read-only memory (EPROM) chips downhole for nonvolatile data storage. The downhole data-acquisition systems are synchronized with a system on the rig that monitors time and drilling depth. On completion of drilling, the drill string was retrieved and the data were downloaded from each tool via a RS232 serial link to a personal computer. The Integrated Drilling Evaluation and Logging (IDEAL) system combines the files and generates ASCII, log information standard (LIS), and digital log information standard (DLIS) data files. This system was also used for post-acquisition data correction and analysis. Further processing was conducted after the cruise at LDEO-BRG and other research centers. These post-cruise processed logging data are available on CD-ROM (back pocket, this volume).

Compensated Dual Resistivity Tool

The CDR tool is similar in principle to the conventional wireline induction tool that measures formation conductivity. A 2-MHz elec-

tromagnetic wave is transmitted, and two receivers detect the signal. The phase shift and amplitude attenuation of the transmitted signal are calculated.

The CDR tool includes a phase caliper, which uses an algorithm to transform the phase sum and the phase shift of the two resistivity measurements into the distance of the sensor from the borehole wall. This allows corrections to be made for borehole effects and tool standoff (Anadrill-Schlumberger, 1993).

The resistivity phase shift (R_{ps} or PSR) measurement is equivalent to the spherically focused resistivity log (SFL) on the wireline induction tool. The average depth of investigation of the resistivity phase shift is 75 cm. The resistivity attenuation deep (R_{ad} or ATR) measurement is equivalent to the dual-induction medium measurement, with an average depth of investigation of 125 cm. The maximum vertical resolution of these measurements is 15 cm. Both depths of investigation are dependent primarily on the resistivity of the formation. In this volume, the attenuation measurement will be called "deep resistivity," and the phase shift measurement will be called "shallow resistivity."

A natural gamma-ray tool (NGT) is integrated into the CDR tool. Under controlled penetration rates of ~15 m/hr, reliable spectral data may be obtained. Total gamma-ray counts are binned into five energy bands to determine the amounts of U, Th, and K in the formation. An average rate of penetration (ROP) of 35 m/hr was maintained during Leg 171A drilling. This drilling speed proved adequate for the collection of reliable spectral gamma-ray measurements, which are typically influenced most by low count statistics at high ROPs.

Compensated Density Neutron Tool

The CDN tool is similar in principle to the wireline compensated density and compensated neutron tools. The density section of the tool uses a 1.7-Ci ¹³⁷Cs gamma-ray source in conjunction with two gain-stabilized scintillation detectors to provide a borehole-compensated density measurement. The detectors are located 7 and 14 in below the source. The number of Compton scattering collisions (change in gamma-ray energy by interaction with the formation electrons) is related to the formation density.

Returns of low-energy gamma rays are converted to a photoelectric effect value, measured in barns per electron. The photoelectric effect value depends on electron density and hence responds to bulk density and lithology (Anadrill-Schlumberger, 1993). It is particularly sensitive to low-density, high-porosity zones.

The density source and detectors are positioned behind holes in the fin of a full-gauge clamp-on stabilizer (Fig. 1). This geometry forces the sensors against the borehole wall, thereby reducing the effects of borehole irregularities and drilling. Neutron logs are processed to eliminate the effects of borehole diameter, tool size, temperature, drilling mud hydrogen index (dependent on mud weight, pressure, and temperature), mud and formation salinities, lithology, and other environmental factors (Schlumberger, 1994). The vertical resolution of the density and photoelectric effect measurements is about 15 and 5 cm, respectively.

Neutron porosity measurements are obtained using fast neutrons emitted from a 7.5-Ci americium oxide-beryllium (Am-Be) source. Hydrogen quantities in the formation largely control the rate at which the neutrons slow down to epithermal and thermal energies. The energy of the detected neutrons has an epithermal component because

¹Moore, J.C., Klaus, A., et al., 1998. *Proc. ODP, Init. Repts.*, 171A: College Station, TX (Ocean Drilling Program).

²Shipboard Scientific Party is given in the list preceding the Table of Contents.

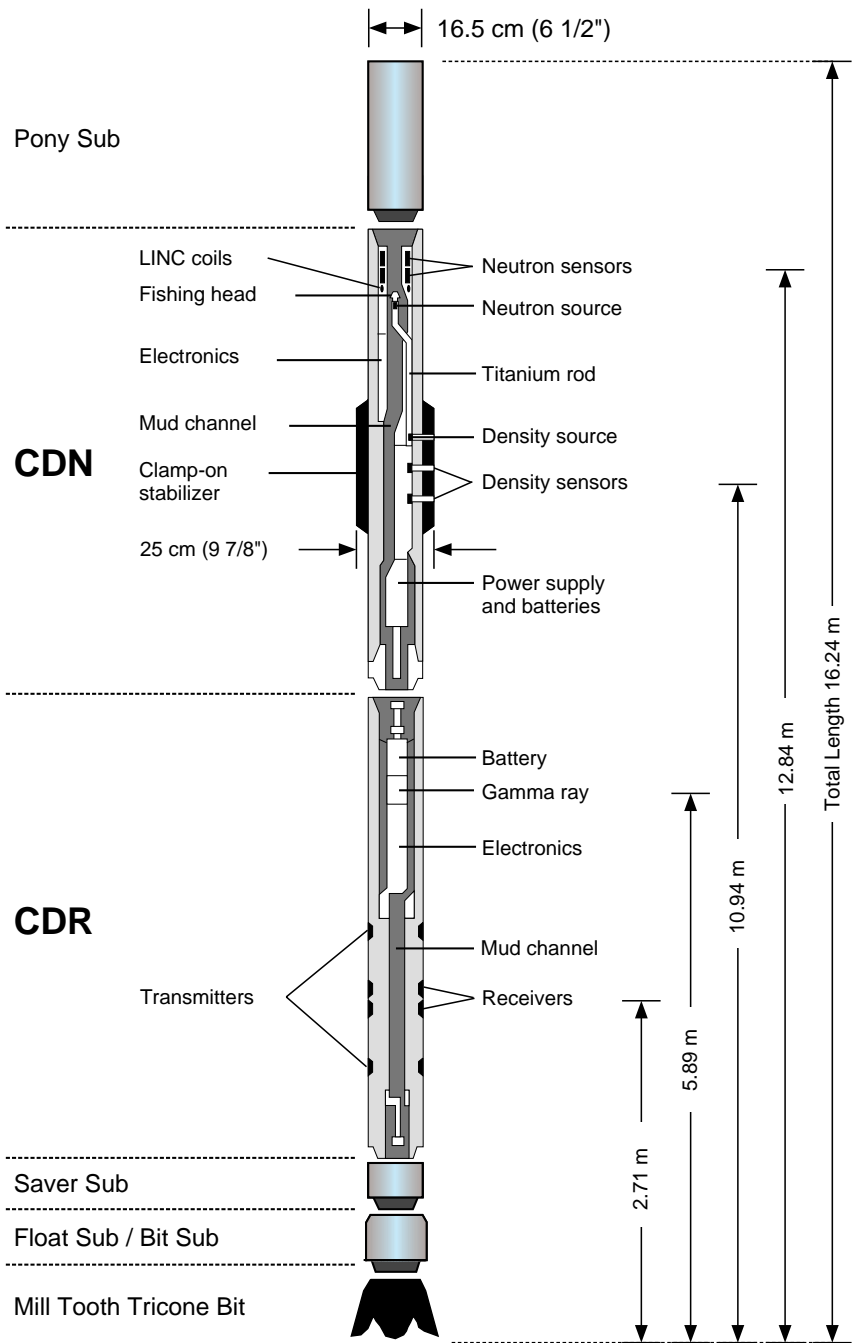


Figure 1. Position and components of the CDR and CDN tools in the drill string used for Leg 171A logging operations.

much of the incoming thermal neutron flux is absorbed as it passes through the 1-in drill collar. Neutrons are detected in near- and far-spacing detector banks, located 9 and 18 in, respectively, above the source. The vertical resolution of the tool under optimum conditions is about 34 cm.

Data output from the CDN tool includes apparent neutron porosity (i.e., the tool does not distinguish between pore water and lattice-bound water), formation bulk density, and photoelectric effect. The density logs presented here have been “rotationally processed” to show the maximum density that the tool reads while it is rotating. In addition, the CDN tool outputs a differential caliper record based on the standard deviation of density measurements made at high sampling rates around the circumference of the borehole. The measured standard deviation is compared with that of an in-gauge borehole, and the difference is converted to the amount of borehole enlargement (Anadrill-Schlumberger, 1993).

A standoff of <1 in between the tool and the borehole wall indicates good borehole conditions, for which the density log values are considered to be accurate to $\pm 0.015 \text{ g/cm}^3$ (Anadrill-Schlumberger, 1993).

Depth Control

Unlike wireline tools, the LWD tools record data in time. The IDEAL surface system records the time and depth of the drill string below the rig floor and ties into the driller’s depth. Although LWD depth control is well established for oil field industry operations, LWD operations aboard the *JOIDES Resolution* require special attention to depth measurements, because drilling is performed without a riser or other fixed reference point, and the ship’s heave cannot be measured directly.

Three optical quadrature phase-shift encoders were installed on the drilling apparatus to measure drawworks movement, heave com-

Table 1. Glossary of borehole logging terms (with units of measurement).

6-in sampling interval
ROP*5 = 5-ft averaged rate of penetration (m/hr)
CDR: compensated dual resistivity
RTIM = resistivity time after bit (s)
GTIM = gamma-ray time after bit (s)
ATR, R_{ad} = deep resistivity (attenuation) (Ωm)
PSR, R_{ps} = shallow resistivity (phase shift) (Ωm)
NGT (part of CDR): natural gamma tool
GR = total gamma ray (GAPI)
SGR = total spectral gamma ray (cps)
CGR = corrected spectral gamma ray (potassium + thorium) (cps)
THOR = thorium (ppm)
Uran = uranium (ppm)
POTA = potassium (wt%)
CDN: compensated density neutron
DC_A = differential caliper (in)
NTAB = neutron time after bit (s)
DTAB = density time after bit (s)
TNPH = thermal neutron porosity (v/v)
PEF = photoelectric effect (barns/electron)
ROMT = density (rotationally processed) (g/cm^3)
DRHO = bulk density correction delta-rho (g/cm^3) = difference between densities computed from "near" and "far" γ -ray receivers
3-in sampling interval
CDR-QRO processed
ATIF = attenuation resistivity, 1-ft resolution
PS1F = phase shift resistivity, 1-ft resolution
1-in sampling interval
CDN = enhanced vertical resolution processed
NROM = resolution enhanced density (actual resolution about 3 in)
Other
LSS = long-spaced sonic tool
VSP = vertical seismic profile
SFL = spherically focused log

Note: Terms in italics are those used to refer to specific logs in the remainder of the volume.

sensor stroke, and top-drive position. Each of these sensors was carefully located and precisely calibrated to give depth measurements with an accuracy >0.1 m. This depth information was written to a file with a time stamp. These data were then passed through a low-pass filter to remove the effects of the high-frequency heave, leaving only the true bit movement.

Synchronization to 1 s of the uphole and downhole clocks allowed merging of the time-depth data (from the surface system) and the downhole time-measurement data (from the tools once returned to surface) into depth-measurement data files, giving data in a format similar to that of conventional wireline logging data.

SEISMIC RESOLUTION AND CORE-LOG-SEISMIC CORRELATION

A primary objective of Leg 171A was to correlate results from previously drilled ODP holes, the 3-D seismic survey, and logs collected during Leg 171A. This suite of observations was acquired over 10 yr, during four different cruises. Critical questions include

1. How accurate was the navigation during each cruise?
2. What was the position of the drill string on the bottom relative to the sea surface, and how large was the hole deviation?
3. How accurate is the depth conversion of the seismic reflection data?
4. What is the inherent resolution of the seismic data?

Navigation

The ODP sites reoccupied during Leg 171A were drilled while the ship was dynamically positioned off an acoustic beacon on the seafloor. The ship's position in dynamic positioning mode was determined by long-term averages of Global Positioning System (GPS)

measurements. Averaging measurements over a period of hours to several days reduces inaccuracies caused by dithering of the GPS signal and any short-term variations caused by the dynamic positioning system's shifting of the drillship. During Leg 110, GPS coverage was not continuous; consequently, these positions were combined with transit satellite locations and were averaged over several days. During Leg 171A, 6-hr GPS averages showed a variation of 2–6 m from the mean GPS location of Site 1044, calculated using all GPS data collected while drilling the site. We assume that this variation is the error in relative location.

The 1992 3-D seismic site survey was navigated by differential GPS. A test of the differential GPS, conducted before the survey while the ship was docked in Barbados, showed that 95% of the fixes taken were within 5 m of the mean. Therefore, the location of any shotpoint that was derived from several smoothed fixes is probably within about 5 m of the actual location. In summary, we believe that the location of the ODP holes and the seismic data have errors <10 m.

Because the bottom of the drill string is not navigated, we do not know its exact position and must therefore assume that it lies directly below the rig floor. During previous drilling, hole deviation information was acquired only from the cores recovered with the advanced hydraulic piston corer (APC) at shallow depths, where it was not significantly different from vertical.

Seismic Resolution

The resolution of the 3-D seismic data used to locate the Leg 171A drill sites is a function mainly of the frequency content of the data (which varies with depth below seafloor) and the velocities used for depth conversion. A primary factor is the inherent frequency content of the seismic data. The seismic data used to locate the sites and to correlate with the log data have a bandwidth of 8–55 Hz and a dominant frequency of 32 Hz. The vertical resolution implied by this frequency band in the depth range of most of the Leg 171A drill holes (i.e., one-quarter of the wavelength of the dominant frequency) is ~ 14 m. The bandwidth of these data also limits the radius of the first Fresnel zone to no less than 387 m. Reflectors at each common midpoint integrate information over this zone. Common midpoints are spaced 15 m east–west by 25 m north–south.

The accuracy of correlating seismic data to the LWD logs is also affected significantly by the uncertainty in the velocities used in the depth migration, which ultimately locates the reflections in depth. Because of the short offset range of these reflection data, a velocity analysis was not possible. Velocities for migration were derived from vertical seismic profile (VSP) results at Sites 948 and 949, velocities from nearby long-offset seismic profiles, and visually selected migration velocities that produced the optimum section (T. Shipley, pers. comm., 1997). The velocity uncertainty is probably <100 to 150 m/s, and thus the vertical precision is no worse than 25 to 37 m.

IDENTIFICATION OF LOGGING UNITS THROUGH VISUAL INTERPRETATION AND MULTIVARIATE STATISTICAL ANALYSIS

Logging units at the Leg 171A sites were defined through a combination of visual interpretation and multivariate statistical analysis. First-order logging units, which are related primarily to lithologic changes, were generally easy to identify visually by examining the character of the gamma-ray, density, thermal neutron porosity, deep resistivity, and photoelectric effect curves. The shallow resistivity data were not used because they correlate strongly with the deep resistivity (i.e., inclusion of the shallow resistivity would weight resistivity too strongly with respect to the remaining data). The uranium log also was not used because it showed little character and contained anomalous negative values. Multivariate statistical analysis provided objective confirmation of the first-order logging unit boundaries and

identified second-order logging units related to more subtle, possibly nonlithologic, trends in the logging data. The multivariate statistical analysis entailed the following steps:

1. Each logging curve was normalized by subtracting the mean and then dividing by the standard deviation. The resulting curves have a mean of zero and a standard deviation of 1.
2. Factors and factor loadings were calculated from the normalized curves using standard R-mode factor analysis procedures, with Kaiser Varimax factor rotation as described, for example, by Davis (1973). Each factor is simply a linear combination of the input variables weighted by the factor loadings; the factors can be visualized as a projection of n input variables (the normalized logging data) onto n linearly independent (uncorrelated) principal axes. Generally, for the Leg 171A LWD data sets, more than 80% of the variance observed in the input variables can be described by the first three factors.
3. The factors were then decimated to a 1-m depth interval using a finite-impulse-response, low-pass antialiasing filter to reduce the number of data points. This step was necessary because of computational limits of the software and hardware used for the next step.
4. Finally, a complete linkage hierarchical cluster analysis (using a Euclidean norm; Davis, 1973) was performed on the three decimated factors that accounted for the greatest percentage of variance observed in the data. This allowed the identification of electrofacies, or logging units, with distinct combinations of logging properties (e.g., Serra, 1986).

Factor analysis is a method of reducing the number of logs without losing important information. Cluster analysis of the three most important factors proved to be a useful and objective method of identifying significant first- and second-order logging units.

CORRELATING LOGGING DATA WITH FLUID-FLOW PATHS

The extensive pore-water chemical analyses from previous drilling legs in the northern Barbados complex can be compared with the LWD data to understand the fluid-flow pathways. Previous drilling legs have identified fluids with exotic chemical and thermal signatures that are localized to faults and sand-rich layers. The chemical composition of the fluids suggests that they may have migrated 50 to 70 km along connected permeable pathways surrounded by sediments of very low permeability (Bekins et al., 1995). The existence of geochemical gradients (Gieskes et al., 1990) and results from flow modeling (Screaton et al., 1990) suggest that flow through the matrix is of minor importance. Thus, most of the flow from deep in the complex is concentrated along discrete pathways that are easily missed by core sampling. To understand the flow system, it is necessary to better characterize these flow pathways.

The location of known fluid-flow pathways is marked by pore waters with low chloride and high methane concentrations, together with isotopic shifts toward increased $\delta^{18}\text{O}$ and δ deuterium values (Gieskes et al., 1990; Vrolijk et al., 1990). In some locations there are also thermal anomalies, but these are less prevalent because they decay more quickly than chemical anomalies (Fisher and Hounslow, 1990). By examining the LWD data in the vicinity of known fluid-flow pathways, it may be possible to determine if they have a characteristic log signature. For example, in some cases geochemical anomalies and associated flow are correlated with sand layers. The LWD data will better define the location, thickness, and porosity of the sand layers. By comparing these data with the geochemical data, it may be possible to better characterize the thickness and permeability of the sand layers that support active flow. Where geochemical analyses are

not available, the LWD data can be used to identify similar high-permeability sands that may constitute other fluid paths.

Where chemical anomalies are associated with faults, the LWD data may indicate other characteristics, such as changes in porosity or bulk density representing dilated cracks or mud-filled veins. Such correlation apparently occurs along the décollement zone at Site 948 (Shipboard Scientific Party, 1995). These physical changes are postulated to be caused by high pore pressures in the vicinity of the fault (Moore and Vrolijk, 1992). For this report, we express these pressures in terms of λ^* :

$$\lambda^* = (P_p - P_h)/(P_l - P_h),$$

where P_p = pore pressure, P_l = lithostatic pressure, and P_h = hydrostatic pressure. The goal is to better characterize the LWD signature wherever it coincides with known chemical anomalies. The LWD data can then be used to identify other faults with possible active flow where chemical data are not available. In addition, in most cases there may be no pore-water chemical sample located at the center of the suspected concentrated flow. The LWD data may be able to pinpoint the center of flow associated with a diffuse chemical anomaly associated with a nearby sample.

DETERMINATION OF RESISTIVITY POROSITY

Resistivity-based porosity was determined using Archie's law (Dewan, 1983; Doveton, 1986):

$$\phi^m = a/FF,$$

where FF is the formation factor. First, a resistivity of water log was created from temperature measurements, salinity, and Schlumberger log interpretation chart Gen-9 (Schlumberger, 1994). Next, a formation factor log was created, where

$$FF = R_o/R_w.$$

R_o is the resistivity of the formation and R_w is the resistivity of the water. Archie's coefficients a and m were found by performing a linear regression on a crossplot of $\ln(FF)$ vs. $\ln(\text{density porosity})$, where $m = -\text{slope}$ and $a = \exp(\text{intercept})$ of the line. Archie's coefficients and the formation factor were then used to create a resistivity porosity log.

The deep resistivity log was used to calculate the resistivity porosity log, because the deeper penetration makes the resistivities more likely to be those of the undisturbed sediment. The advantages of the resistivity porosity log over a porosity log derived from the density log are that the grain density need not be known and the deep resistivity log is less sensitive than the density log to variations in borehole diameter. Nevertheless, because Archie's law is not applicable to a conducting clay matrix, the resistivity porosity log is unlikely to be accurate at many of the sites.

SEISMIC WAVEFORM MODELING

Synthetic seismograms were constructed from the LWD density log for correlation of the LWD data with the 3-D seismic reflection records. Seismic impedance for the synthetic trace was calculated assuming a linear increase in velocity through each of three intervals drilled on Leg 171A: the accretionary complex, the underthrust sequence, and the stratigraphic sequence seaward of the deformation front. The assumptions about the velocity gradients are necessary because no sonic log exists for any of these holes. With the continuous,

linear velocity profile, impedance contrasts are a product of changes in density with depth only and are largely unaffected by the assumed velocities. The density log was filtered with a Gaussian filter and resampled at 2-m intervals before calculation of the reflection coefficients. The reflection coefficient series was converted to time using the linear velocity profile and was then resampled at 2-ms intervals. The reflection coefficients were convolved with a source derived from stacking seafloor reflections from the undeformed seafloor sequence east of the deformation front. The same source wavelet was used for the synthetic seismogram generated at each site. The synthetic trace was then converted back to depth for display purposes.

REFERENCES

- Anadrill-Schlumberger, 1993. *Logging While Drilling*: Houston (Schlumberger), document SMP-9160.
- Bekins, B.A., McCaffrey, A.M., and Driess, S.J., 1995. Episodic and constant flow models for the origin of low-chloride waters in a modern accretionary complex. *Water Resour. Res.*, 31:3205–3215.
- Davis, J.C., 1973. *Statistics and Data Analysis in Geology*: New York (Wiley).
- Desbrandes, R., 1994. *Data Acquisition and Processing While Drilling*: Dept. Petrol. Eng., Louisiana State Univ.
- Dewan, J.T., 1983. *Essentials of Modern Open-Hole Log Interpretation*: Tulsa (PennWell).
- Doveton, J.H., 1986. *Log Analysis of Subsurface Geology: Concepts and Computer Methods*: New York (Wiley).
- Fisher, A.T., and Hounslow, M.W., 1990. Heat flow through the toe of the Barbados accretionary complex. In Moore, J.C., Mascle, A., et al., *Proc. ODP, Sci. Results*, 110: College Station, TX (Ocean Drilling Program), 345–363.
- Gieskes, J.M., Vrolijk, P., and Blanc, G., 1990. Hydrogeochemistry of the northern Barbados accretionary complex transect: Ocean Drilling Program Leg 110. *J. Geophys. Res.*, 95:8809–8818.
- Moore, J.C., and Vrolijk, P., 1992. Fluids in accretionary prisms. *Rev. Geophys.*, 30:113–135.
- Schlumberger, Inc., 1994. *Log Interpretation Charts*: Houston (Schlumberger).
- Screaton, E.J., Wuthrich, D.R., and Driess, S.J., 1990. Permeabilities, fluid pressures, and flow rates in the Barbados Ridge Complex. *J. Geophys. Res.*, 95:8997–9007.
- Serra, O., 1986. *Fundamentals of Well-Log Interpretation* (Vol. 2): *The Interpretation of Logging Data*. Dev. Pet. Sci., 15B.
- Shipboard Scientific Party, 1995. Site 948. In Shipley, T.H., Ogawa, Y., Blum, P., et al., *Proc. ODP, Init. Repts.*, 156: College Station, TX (Ocean Drilling Program), 87–192.
- Shipley, T.H., Ogawa, Y., Blum, P., et al., 1995. *Proc. ODP, Init. Repts.*, 156: College Station, TX (Ocean Drilling Program).
- Silver, E., Kimura, G., Blum, P., et al., 1997. *Proc. ODP, Init. Repts.*, 170: College Station, TX (Ocean Drilling Program).
- Vrolijk, P., Chambers, S.R., Gieskes, J.M., and O'Neil, J.R., 1990. Stable isotope ratios of interstitial fluids from the Northern Barbados Accretionary Prism, ODP Leg 110. In Moore, J.C., Mascle, A., et al., *Proc. ODP, Sci. Results*, 110: College Station, TX (Ocean Drilling Program), 189–205.
- Wraight, P., Evans, M., Marienback, E., Rhein-Knudsen, E.M., and Best, D., 1989. Combination formation density and neutron porosity measurements while drilling. *Trans. SPWLA 30th Ann. Logging Symp.*, Denver.

Ms 171AIR-102